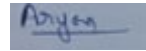


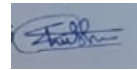
Development of Acoustophoretic Printer and Study of Droplet Formation

Project Number D9

Aryan Goel - 2022ME11990

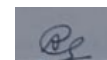


Shubham Kurre – 2022ME11325

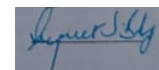


Department of Mechanical Engineering
Indian Institute of Technology Delhi

Supervisor – Prof. Arpan Gupta



Co- Supervisor – Prof. Supreet Singh Bahga



Mid-term report

Abstract:

The development of an acoustophoretic printer addresses the significant challenge of printing high-viscosity liquids, a limitation faced by traditional inkjet and electrohydrodynamic printing techniques which are heavily influenced by fluid viscosity. Acoustophoretic printing utilizes acoustic radiation forces to achieve contactless and nozzle-free droplet ejection, rendering the process largely independent of viscous forces. This innovation enables precise droplet generation from fluids with a wide range of viscosities, including bio-inks, pharmaceutical solutions, soft electronics materials, and other functional fluids.

- **Objectives:** The primary objectives of this project are to design and fabricate an acoustophoretic printing system that integrates a subwavelength acoustic resonator with a CNC 3018 machine and microscope-based imaging setup, conduct controlled droplet generation experiments under quasi-static and acoustic conditions, and characterize droplet size distribution and ejection dynamics. The project also aims to perform acoustic field simulations and optimize printing parameters such as frequency, power, and nozzle geometry.
- **Work completed so far:** It includes a comprehensive literature review of acoustic droplet generation techniques and resonator designs. The CNC 3018 machine was customized and assembled, involving removal of the stock spindle and installation of mounts for nozzles and microscope setup. Calibration was performed using needle diameter measurements with an electronic vernier calliper to convert microscope image pixels to real-world lengths. Quasi-static experiments were conducted with three needle sizes and multiple fluids including water, sunflower oil, and glycerol. Droplet formation was recorded via high-resolution imaging and videos, followed by image processing in MATLAB to measure droplet diameters accurately. Challenges such as droplet stabilization and image thresholding were addressed through iterative improvements.
- **Future work plan:** It includes the CAD modelling and fabrication of an acoustic resonator chamber, integration of the resonator with the transducer and CNC setup. Subsequent acoustophoretic printing experiments will test water-glycerol mixtures first, followed by high-viscosity fluids such as polyethylene glycol solutions, honey, and resins. Calibration experiments will investigate the effects of acoustic parameters on droplet size and ejection consistency. The project timeline concludes with comparative analysis of quasi-static versus acoustic droplet ejection, data compilation, and final report preparation.

Table of Contents:

Chapter 1: Introduction	3
Chapter 2: Literature Review	4
Chapter 3: Methodology.....	6
Chapter 4: Current Progress.....	8
Chapter 5: Remaining Work and Plan	19
Chapter 6: Conclusions.....	21
References.....	22

Chapter 1: Introduction

1.1 Background & Context

Traditional printing techniques face challenges when dealing with high-viscosity liquids due to their dependence on fluid properties like viscosity. Acoustophoretic printing offers a novel solution by using acoustic radiation forces to enable contactless, nozzle-free droplet ejection. This approach allows printing of a wide range of fluids with varying viscosities, making it suitable for advanced applications in biotechnology, electronics, and additive manufacturing.

1.2 Objectives

The primary objectives of this project are to:

- Design and develop an acoustophoretic printing system integrating an acoustic resonator with a CNC-based platform for controlled droplet ejection.
- Experimentally characterize droplet formation under quasi-static conditions using varied nozzle sizes and fluid types.
- Fabricate and optimize an acoustic resonator tuned to operate near 25 kHz for effective acoustophoretic droplet generation.
- Validate printing performance through acoustophoretic ejection and study the effects of acoustic parameters on droplet size and consistency.

1.3 Structure of the Report

This report presents a comprehensive overview of the project, beginning with the background and motivation followed by a review of relevant literature. It then details the experimental methodology and the setup for quasi-static droplet measurements, along with calibration and data analysis procedures. The report also discusses the progress made so far and challenges faced, before outlining the plan for completing the acoustophoretic printing system and future testing plans.

Chapter 2: Literature Review

The development of acoustophoretic printers has emerged as a promising alternative to conventional droplet-based printing methods such as inkjet and extrusion. Unlike nozzle-driven systems, acoustophoretic printing relies on acoustic forces to manipulate fluids and particles in a contactless manner, enabling precise droplet generation across a wide range of material properties. This section reviews the key technological advancements, system designs, performance metrics, and application areas reported in the literature.

2.1 Acoustic Principles and Printing Mechanisms

The earliest demonstrations of acoustic ink printing were reported by Hadimioglu et al. (1992, 2001) [1], who developed nozzle less systems using focused acoustic beams and thin-film zinc oxide (ZnO) transducers. These systems were capable of ejecting droplets as small as 1.5 picolitres at frequencies up to 25 kHz, achieving resolutions of 600 spots per inch suitable for photographic-quality printing. Subsequent innovations explored a wider range of acoustic manipulation mechanisms, including subwavelength Fabry–Perot resonators (Foresti et al., 2018) [2], phased-array acoustic levitation (Chen et al., 2024) [3], piezoelectric focusing in microchannels (Leibacher et al., 2015) [4], and gigahertz-scale resonators for single-cell manipulation (Zhou et al., 2021) [5]. These approaches highlight the versatility of acoustics in enabling droplet formation, levitation, or focusing without reliance on nozzles.

2.2 System Designs and Components

Reported system architectures vary significantly depending on the target application. Ink printing systems often employ ZnO or PZT transducers combined with Fresnel or silicon lenses for droplet focusing (Hadimioglu et al., 1992, 2001) [1]. More recent bioprinting platforms integrate microfluidic nozzles with piezoelectric elements to improve bead focusing efficiency (Leibacher et al., 2015) [4]. Foresti et al. (2018) [2] demonstrated the use of magneto strictive transducers coupled with Fabry–Perot resonators for high-viscosity fluid handling, while Chen et al. (2024) [3] advanced

omnidirectional 3D printing through phased-array transducers capable of voxel-by-voxel deposition. These innovations reflect a shift from two-dimensional ink deposition toward complex, contactless additive manufacturing.

2.3 Printing Performance and Material Handling

Performance metrics reported across studies emphasize droplet size control, throughput, and compatibility with diverse materials. Hadimioglu et al. (2001) [1] achieved sub-picolitre droplets with multi-gray level printing, while Foresti et al. (2018) [2] demonstrated droplet diameters tunable between $<65\text{ }\mu\text{m}$ and $>800\text{ }\mu\text{m}$ at ejection rates of $\sim 1000\text{ Hz}$. Chen et al. (2024) [3] extended viscosity handling to the range of $1\text{--}5,000,000\text{ mPa}\cdot\text{s}$, enabling printing of structural, conductive, and biological materials on complex substrates. Liu et al. (2021) [6] introduced the concept of acoustophoretic liquefaction, achieving enhanced resolution ($>25\%$), faster print speeds ($>3\times$), and compatibility with ultrahigh-viscosity nanoparticle suspensions ($>3700\text{ Pa}\cdot\text{s}$).

2.4 Applications in Bioprinting and Single-Cell Manipulation

One of the most significant areas of application for acoustophoretic printing is bioprinting. Zhou et al. (2021) [5] reported 100% single-cell encapsulation with high spatial precision ($\sim 5\text{ }\mu\text{m}$), while Chen et al. (2021) [3] demonstrated nozzle-free acoustic droplet ejection for constructing tumor microenvironments with cell viability exceeding 94%. Similarly, Leibacher et al. (2015) [4] achieved 95.6% single-bead efficiency and 99% bead focusing, highlighting the technology's potential in single-cell studies. Foresti et al. (2018) [2] and Nguyen (2018) extended applications to the patterning of viscous bioinks, food, and hydrogels, underscoring the ability of acoustophoretic printers to handle high-viscosity and cell-laden materials without compromising viability.

Chapter 3: Methodology

The experimental platform is built on a modified CNC 3018 machine, which provides precise control over the vertical position of the nozzle. The stock spindle was replaced with a custom 3D-printed mount to securely hold varying needle sizes. A high-resolution digital microscope was mounted onto a stable, vibration-isolated base, allowing clear imaging and real-time monitoring of droplet formation. LED lighting was attached to the microscope to enhance droplet visibility and eliminate glare. The system was aligned so the microscope's field of view coincided with the needle tip for repeatable imaging and data collection.

Three fluids—deionized water, refined sunflower oil, and glycerol—were selected to represent a physical spectrum of viscosity and surface tension. Experiments were conducted for three different needle gauges (18G, 22G, 25G). For each fluid and needle combination, three trials were performed, and each droplet was imaged and measured independently, ensuring statistical robustness and repeatability.

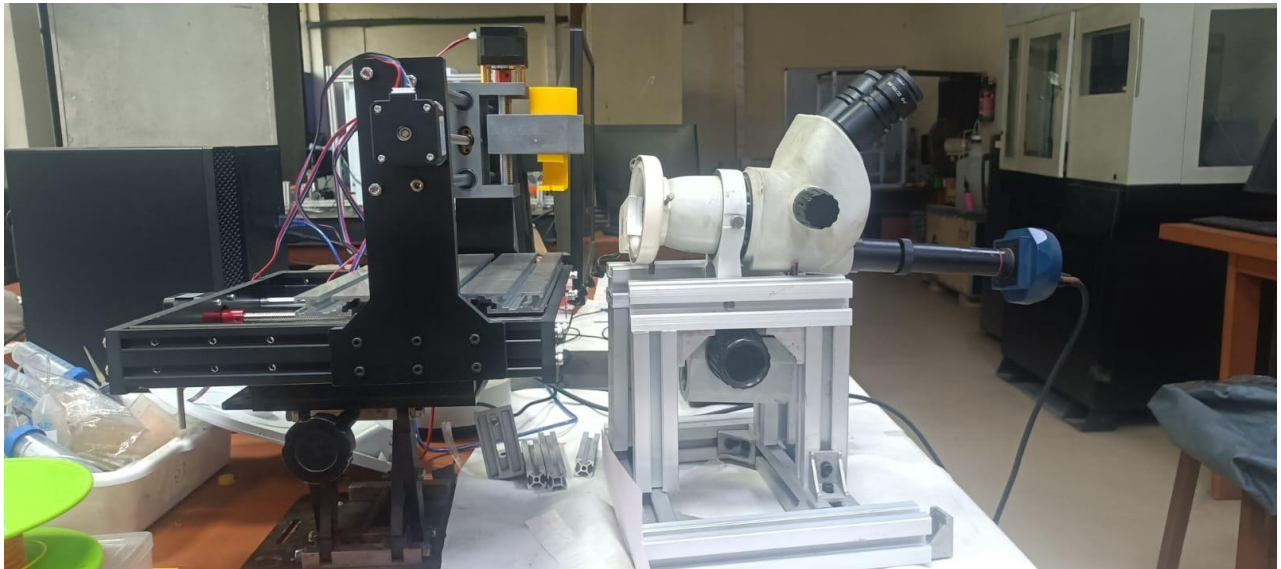


Fig 1. Complete Setup with CNC integrated with mount and microscope fixed



Fig 2. 3D Mount with Needle



Fig 3. Syrine Carrying Liquid

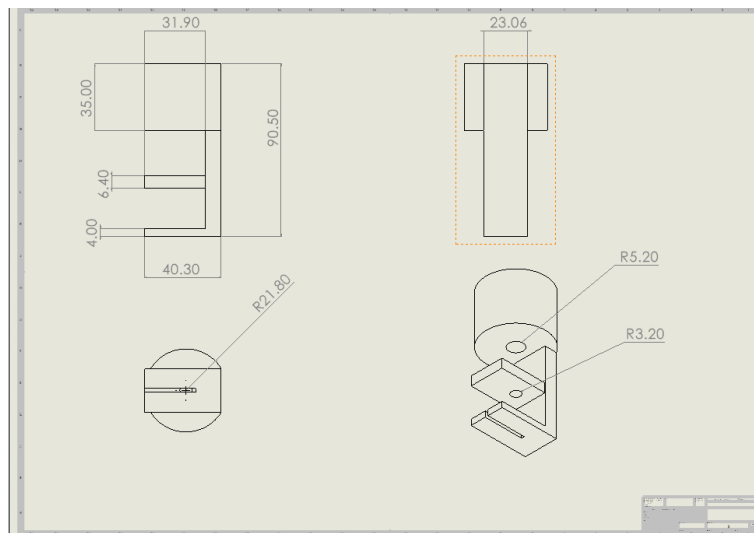


Fig 4. Parametric View Of 3D Mount

Chapter 4: Current Progress

4.1 Experimental Setup and Calibration

The experimental setup involved a modified CNC 3018 machine, where the stock spindle was removed and replaced with a custom mount to hold various needle nozzles securely. A high-resolution microscope was installed on a vibration-isolated platform to capture clear images and videos of the droplet formation process. The microscope's field of view was meticulously aligned with the nozzle tip to ensure accurate observation.

Calibration was a critical step, performed by measuring the precise diameter of each needle with an electronic vernier calliper. This measurement established the reference scale to convert microscope image pixels into actual physical dimensions. The alignment of the droplet under the microscope, lighting conditions, and image clarity were optimized through repeated trials.

4.2 Fluids and Needle Sizes

Experiments were conducted using three different fluids: water, sunflower oil, and glycerol, selected for their varied viscosities and surface tensions. Three needle sizes were used: 18-gauge (1.26 mm), 22 gauge (0.71 mm), and 25 gauge (0.49 mm), to observe the influence of nozzle diameter on droplet formation. For each needle-fluid combination, three trials were performed to ensure repeatability and statistical validity in the measurements.

4.3 Data Acquisition and Analysis

Droplet formation was recorded both as high-resolution images and videos using the microscope connected to a computer. The MATLAB software was employed to process the images through pixel counting techniques, translating the visual data into quantitative droplet diameter measurements.

Furthermore, theoretical droplet diameters were estimated by balancing surface tension and gravitational forces, providing a baseline for comparison with experimental data. Surface tension measurements were also conducted using pendant drop analysis in ImageJ software, especially for glycerol, to complement the droplet size studies.

4.4 Quantitative Results

4.4.1 Deionized Water:

Trial No.	Needle Width (Gauge)	D1(pixels)	D2(pixels)	$D_{avg} = (D1 + D2)/2$ (pixels)
1	18	793	634	713
2	18	793	623	708
3	18	767	616	691
1	22	550	509	529
2	22	539	502	520
3	22	527	494	511
1	25	524	487	505
2	25	535	491	513
3	25	513	484	498

Needle Width (Gauge)	Needle Width(pixels)	$D_{avg} = (D_{avg, trial1} + D_{avg, trial2} + D_{avg, trial3})/3$ (pixels)	Diameter of droplet obtained experimentally (mm)
18	243	704	3.65
22	136	520	2.71
25	92	505	2.69

Surface Tension = 72 mN/m

Density = 1000 kg/m³

Under Quasi- Static Conditions:

$$D = \left(\frac{6\sigma d}{\rho g} \right)^{\frac{1}{3}}$$

Where D is theoretical Diameter of droplet in mm,

d is needle width in mm,

σ is surface tension in N/m,

ρ is density in Kg/m³.

Which gives $D_{\text{theoretical}} = 3.53 d^{\frac{1}{3}}$.

For reference, the horizontal diameter is taken as D2 and vertical as D1.

4.4.2 Refined Sunflower Oil:

Trial No.	Needle Width (Gauge)	D1(pixels)	D2(pixels)	$D_{avg} = (D1 + D2)/2$ (pixels)
1	18	646	476	561
2	18	601	468	535
3	18	623	487	555
1	22	527	424	476
2	22	524	421	472
3	22	521	421	471
1	25	439	354	397
2	25	417	377	397
3	25	417	380	398

Needle Width (Gauge)	Needle Width(pixels)	$D_{avg} = (D_{avg, trial1} + D_{avg, trial2} + D_{avg, trial3})/3$ (pixels)	Diameter of droplet obtained experimentally (mm)
18	255	550	2.71
22	140	473	2.40
25	103	397	1.89

Surface Tension = 33.5 mN/m

Density = 915.6 kg/m³

Under Quasi- Static Conditions:

$$D = \left(\frac{6\sigma d}{\rho g} \right)^{\frac{1}{3}}$$

Where D is theoretical Diameter of droplet in mm,

d is needle width in mm,

σ is surface tension in N/m,

ρ is density in Kg/m³.

Which gives $D_{\text{theoretical}} = 2.81 d^{\frac{1}{3}}$.

4.4.3 Glycerol

Trial No.	Needle Width (Gauge)	D1(pixels)	D2(pixels)	$D_{avg} = (D1 + D2)/2$ (pixels)
1	18	638	472	555
2	18	649	476	563
3	18	668	498	583
1	22	520	465	492
2	22	539	472	505
3	22	535	480	507
1	25	406	377	391
2	25	432	395	413
3	25	428	398	413

Needle Width (Gauge)	Needle Width(pixels)	$D_{avg} = (D_{avg, trial1} + D_{avg, trial2} + D_{avg, trial3})/3$ (pixels)	Diameter of droplet obtained experimentally (mm)
18	236	567	3.03
22	133	502	2.68
25	92	406	2.16

Surface Tension = 64 mN/m

Density = 1371 kg/m³

Under Quasi- Static Conditions:

$$D = \left(\frac{6\sigma d}{\rho g} \right)^{\frac{1}{3}}$$

Where D is theoretical Diameter of droplet in mm,

d is needle width in mm,

σ is surface tension in N/m,

ρ is density in Kg/m³.

Which gives $D_{\text{theoretical}} = 3.05 d^{\frac{1}{3}}$.

4.5 Qualitative Results:

4.5.1 Deionized Water:

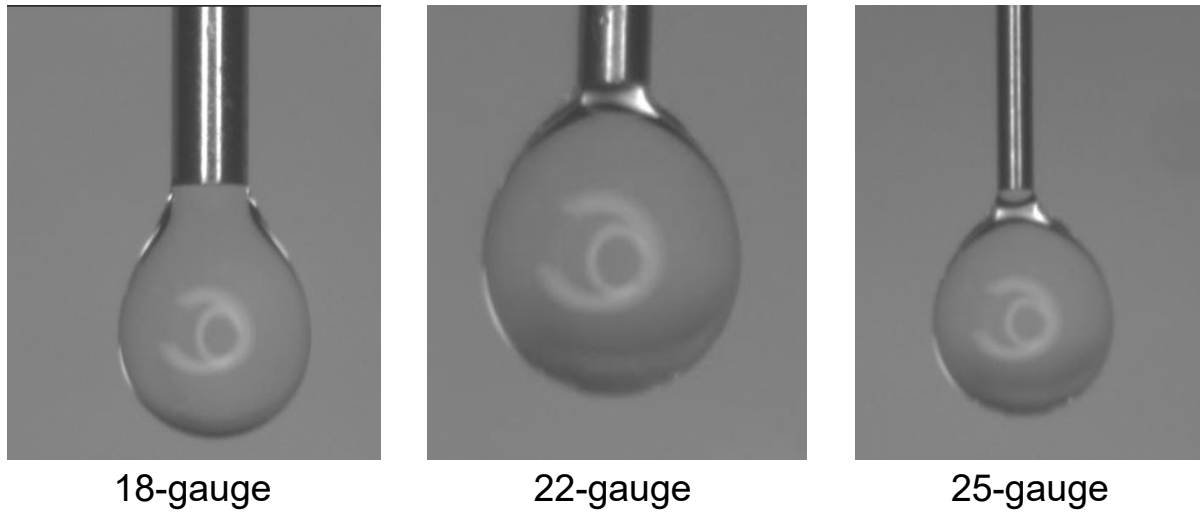


Fig 1. Drop measurement for deionized water

4.5.2 Refined Sunflower Oil:

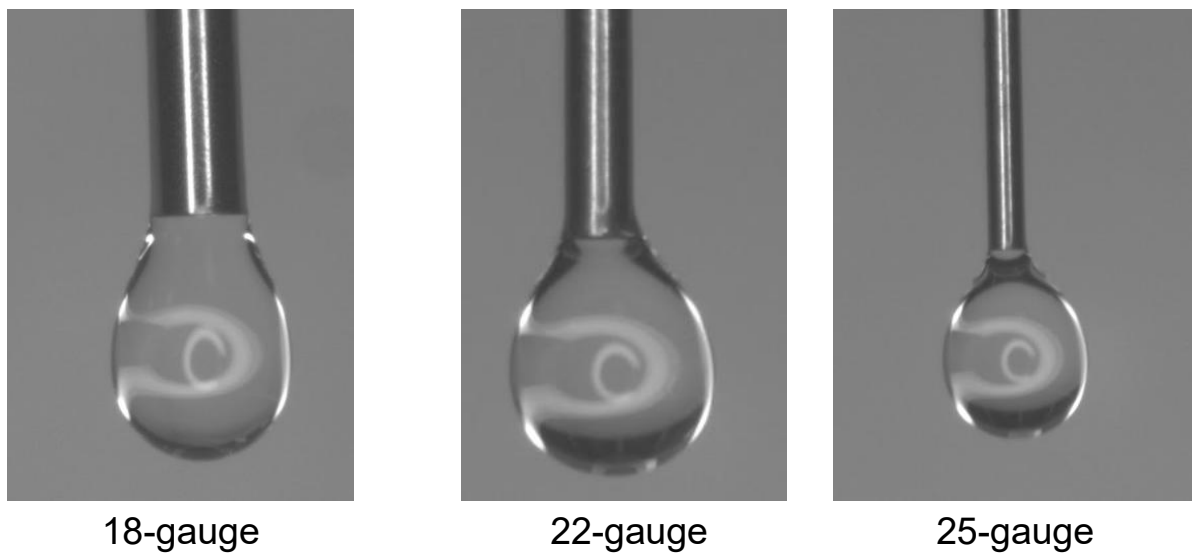


Fig 2. Drop measurement for refined sunflower oil

4.5.3 Glycerol:

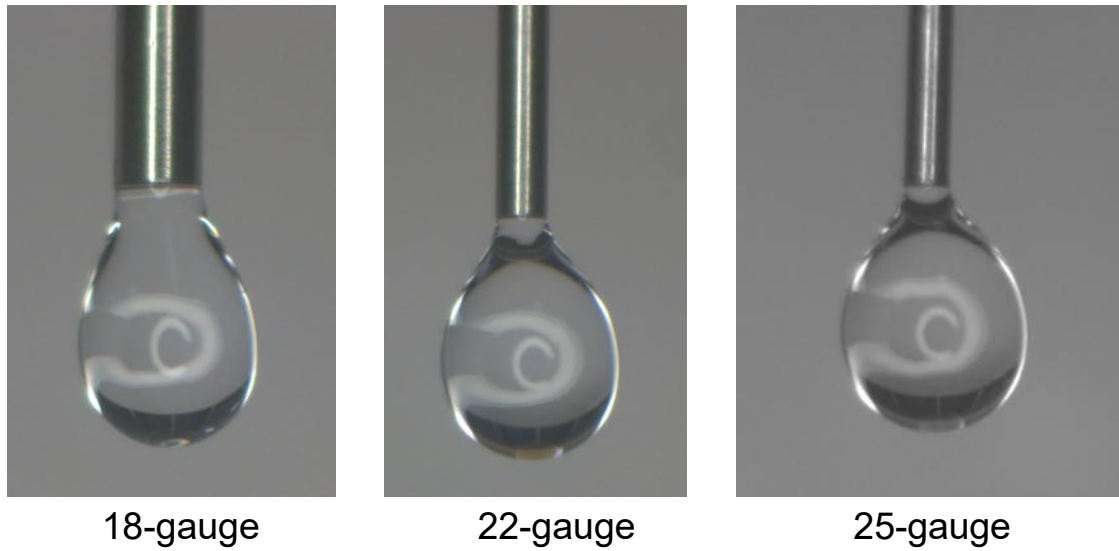


Fig 3. Drop measurement for glycerol

4.5.4 Dimensionless plot for all three liquids:

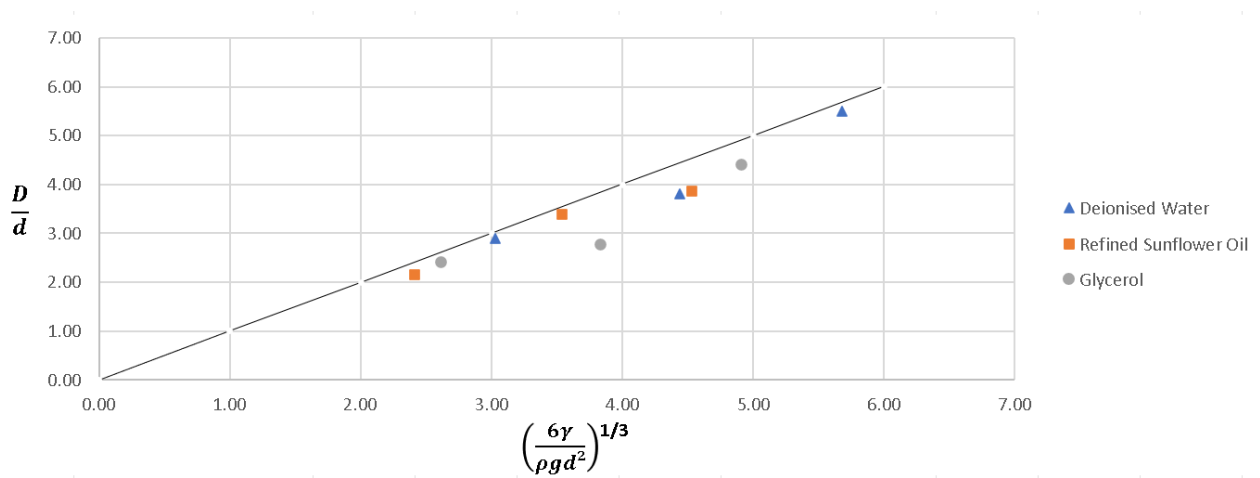


Fig 4. Dimensionless Plot to compare theoretical and experimental results

4.5.5 MATLAB Code:

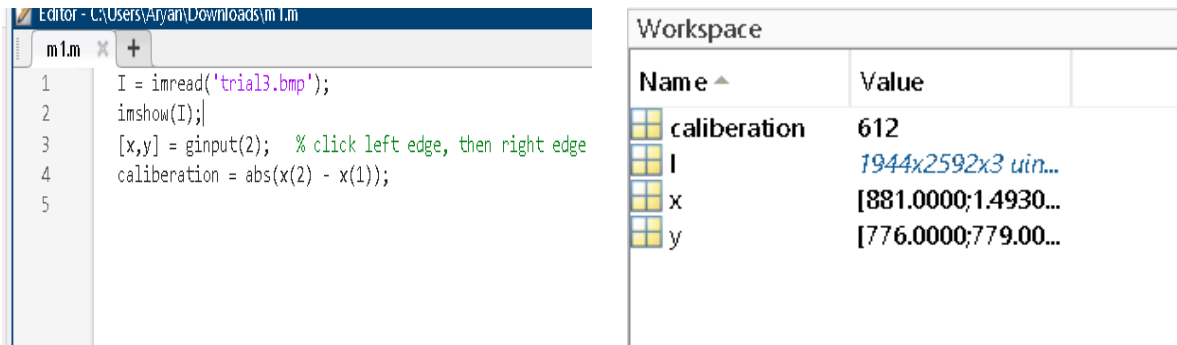


Fig 5: MATLAB Code to count pixels of droplet

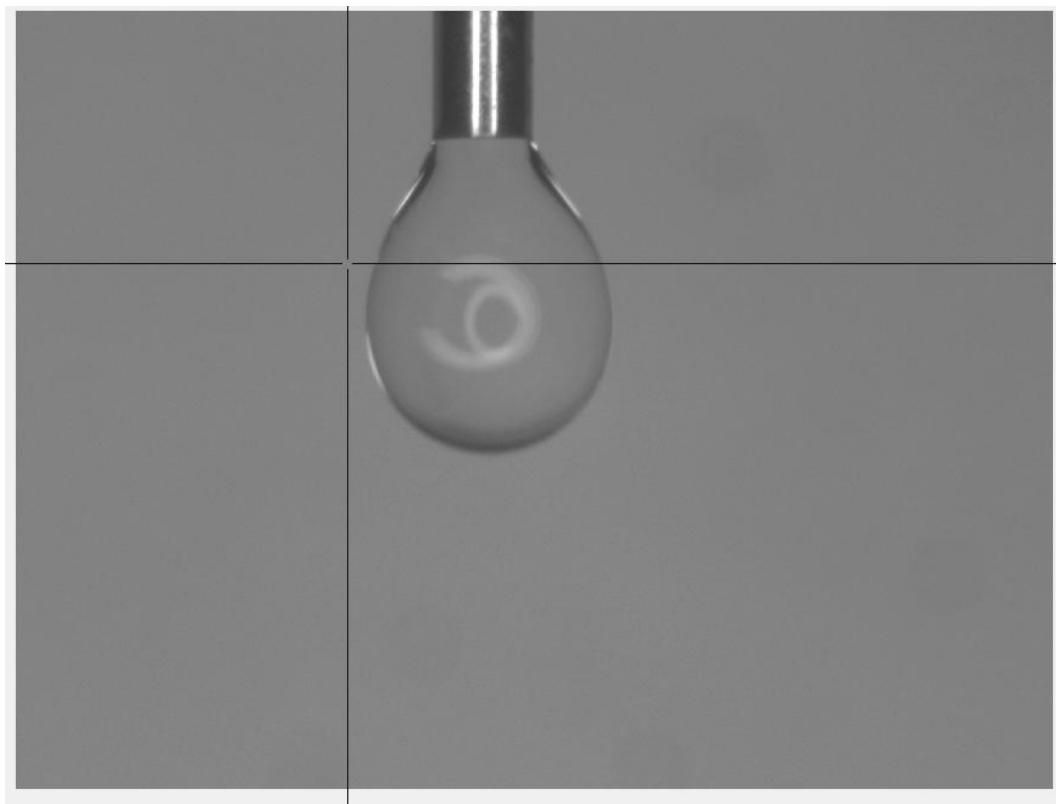


Fig 6. MATLAB window showing how edges are selected

4.6 Key Observations

- Droplet diameter decreases with increasing needle gauge (smaller internal diameter).
- Droplet diameter is not dependent on viscosity as experiment is done under quasi-static conditions.
- The empirical and theoretical correlations used agree well with experimental measurements, confirming the overall approach.

4.7 Challenges and Mitigation

- **Repeatability:** Ensuring a stable quasi-static droplet before detachment required multiple trials; averaged readings were taken to minimise error.
- **Needle diameter verification:** Actual inner diameters were measured using a micrometre to reduce uncertainty in theoretical calculations.
- **Ambient conditions:** Experiments were performed in a controlled environment to limit temperature-induced changes in surface tension.

Chapter 5: Remaining Work & Plan

The next phase of the project will focus on developing and validating the acoustophoretic printing setup. The plan covers both technical milestones and experimental deliverables as mapped in the 12-week Gantt chart.

Key upcoming tasks include:

- **CAD modelling and fabrication of the acoustic resonator:** Creating a resonator design optimized for 25 kHz operation and fabricating chamber components.
- **Resonator system assembly and integration:** Assembling the resonator and transducer, and integrating them with the CNC platform for full system operation.
- **Acoustic field simulations:** Using tools such as ANSYS to simulate and optimize pressure fields and resonator dimensions for efficient droplet ejection.
- **Initial acoustophoretic trials:** Conducting first experiments with water-glycerol mixtures to visualize and validate acoustic droplet ejection.
- **Calibration experiments:** Systematically varying control parameters (acoustic frequency, input power, nozzle size) to generate calibration curves of droplet size and ejection rate.
- **Extended trials with high-viscosity fluids:** Applying the acoustophoretic system to challenging fluids (PEG, honey, resins), quantifying performance and repeatability.
- **Comparative analysis and final reporting:** Comparing quasi-static and acoustophoretic results, compiling data, and preparing the final report and presentation.

Gantt Chart for Remaining Work:

Task	Week 6	Week 7	Week 8	Week 9	Week 10
CAD modeling of resonator (subWAVE)					
Fabrication & assembly of resonator chamber					
System integration: resonator + transducer + CNC					
First acoustophoretic trials (water/glycerol)					
Acoustic field simulation (ANSYS)					
Extended viscosity tests (PEG, honey, resins)					
Calibration experiments (frequency, power, nozzle size)					

Chapter 6: Conclusions

This mid-term report documents substantial progress towards developing an acoustophoretic printing system designed to overcome the limitations encountered in printing high-viscosity liquids. Experimental work has successfully established a robust baseline for droplet formation under quasi-static conditions using multiple needle sizes and fluids. The quantitative and qualitative analyses have validated the experimental setup, calibration methods, and analytical models, confirming good agreement between theory and results.

Several key findings emerged: droplet size is strongly influenced by both needle gauge and fluid surface tension, with repeatable trends observed in all trials. Technical challenges, specifically in calibration, alignment, and imaging, were systematically addressed, improving experimental accuracy and reliability. The methodology has been refined through this initial phase and is now well-positioned for transition to true acoustophoretic trials.

Lessons learned include the importance of precise calibration, systematic data acquisition, and clear visualization techniques for reliable droplet analysis. These insights will guide the assembly and testing of the acoustic printing setup, ensuring an efficient and rigorous approach in the project's second half.

Overall, the work completed lays a strong foundation for the remaining research and development tasks. The team is prepared to begin fabrication, acoustic testing, and comparative analysis of the full system, advancing toward the project's objective of viscosity-independent droplet printing.

References:

- [1] B. Hadimioglu *et al.*, “Acoustic ink printing,” in *Proc. IEEE Ultrason. Symp.*, Institute of Electrical and Electronics Engineers Inc., 1992, pp. 929–935. doi: 10.1109/ULTSYM.1992.275823.
- [2] D. Foresti *et al.*, “Acoustophoretic printing,” *Sci. Adv.*, vol. 4, no. 8, 2018, doi: 10.1126/sciadv.aat1659.
- [3] H. Chen *et al.*, “Omnidirectional and Multi-Material In Situ 3D Printing Using Acoustic Levitation,” *Adv. Mater. Technol.*, vol. 10, no. 9, 2025, doi: 10.1002/admt.202401792.
- [4] I. Leibacher, J. Schoendube, J. Dual, R. Zengerle, and P. Koltay, “Enhanced single-cell printing by acoustophoretic cell focusing,” *Biomicrofluidics*, vol. 9, no. 2, 2015, doi: 10.1063/1.4916780.
- [5] Y. Zhou, M. He, and X. Duan, “100% Single Cell Encapsulation via Acoustofluidic Printing Based on a Gigahertz Acoustic Resonator,” in *Proc. Annu. Int. Conf. IEEE Eng. Med. Biol. Soc. EMBS*, Institute of Electrical and Electronics Engineers Inc., 2021, pp. 1172–1175. doi: 10.1109/EMBC46164.2021.9631051.
- [6] Z. Liu *et al.*, “Acoustophoretic Liquefaction for 3D Printing Ultrahigh-Viscosity Nanoparticle Suspensions,” *Adv. Mater.*, vol. 34, no. 7, 2022, doi: 10.1002/adma.202106183.